Scientific Research Publishing

American Journal of Plant Sciences, 2021, 12, 53-70
https://www.scirp.org/journal/ajps
ISSN Online: 2158-2750
ISSN Print: 2158-2742

Further Insights on the *Datura innoxia* Hyoscyamine 6*β*-Hydroxylase (DiH6H) Based on Biochemical Characterization and Molecular Modeling

Daniel Schlesinger[1,2], Faris Salama[3], Rachel Davidovich Rikanati[2], Rotem Sertchook[4], Ofir Tal[2], Mosaab Yahyaa[2], Adi Faigenboim[3], Mwafaq Ibdah[2], Moshe Inbar[1], Efraim Lewinsohn[2,5*]

[1]Department of Evolutionary & Environmental Biology, University of Haifa, Haifa, Israel
[2]Department of Vegetable Crops Newe Ya'ar Research Center, Agricultural Research Organization, Ramat Yishay, Israel
[3]Institute of Plant Sciences, Agriculture Research Organization, RishonLe Zion, Israel
[4]Lilienblum 3, Gedera, Israel
[5]Department of Vegetable Crops, The Robert Smith Faculty of Agriculture, The Hebrew University of Jerusalem, Rehovot, Israel
Email: dschlez@gmail.com, faris.salama@gmail.com, davidovi@volcani.agri.gov.il, rotem.sertchook@gmail.com, ofirt@volcani.agri.gov.il,mosab_yahya@hotmail.com,adif@volcani.agri.gov.il, mwafaq@volcani.agri.gov.il, minbar@research.haifa.ac.il, *twefraim@volcani.agri.gov.il

How to cite this paper: Schlesinger, D., Salama, F., Rikanati, R.D., Sertchook, R., Tal, O., Yahyaa, M., Faigenboim, A., Ibdah, M., Inbar, M. and Lewinsohn, E. (2021) Further Insights on the *Datura innoxia* Hyoscyamine 6*β*-Hydroxylase (DiH6H) Based on Biochemical Characterization and Molecular Modeling. *American Journal of Plant Sciences*, **12**, 53-70.
https://doi.org/10.4236/ajps.2021.121005

Received: November 19, 2020
Accepted: January 19, 2021
Published: January 22, 2021

Abstract

Hyoscyamine, anisodamine and scopolamine are tropane alkaloids present in some Solanaceae species and used in modern medicine. L-Hyoscyamine is hydroxylated to 6*β*-hydroxyhyoscyamine (anisodamine) and then epoxidated to scopolamine by the dual action of hyoscyamine 6*β*-hydroxylase (H6H), a 2-oxoglutarate dependent dioxygenase. A natural mutation in the Gly-220 residue to Cys was previously shown to be associated with the loss of function of H6H in *Mandragora officinarum*, preventing the accumulation of anisodamine and scopolamine in these plants. We show here that a deliberate Gly220Cys mutation in the *Datura innoxia* DiH6H protein caused a loss of both its enzymatic abilities and rendered it unable to hydroxylate L-hyoscyamine into anisodamine and to epoxidate anisodamine into scopolamine. By using protein modeling based on an available crystal structure of H6H from *Datura metel*, we show how the Cys220 residue causes a steric interference in the active site cavity impairing the interaction of both substrates, hyoscyamine and anisodamine with the active site of the protein. We also address the enantiomeric preference of DiH6H based on molecular modeling.

Keywords

Hyoscyamine 6*β* Hydroxylase, *Datura innoxia*. Mill., Solanaceae,

Scopolamine, Hyoscyamine

1. Introduction

1.1. Hyoscyamine and Scopolamine Are Medicinally Important Tropane Alkaloids Present in the Solanaceae

Hyoscyamine and scopolamine are commercially important tropane alkaloids found in several Solanaceae genera, including *Hyoscyamus*, *Duboisia*, *Scopolia*, *Mandragora*, *Anisodus* and *Datura*. Scopolamine differs from hyoscyamine by the presence of an epoxide bridge in the tropane ring of scopolamine (**Figure 1**). Both hyoscyamine and scopolamine affect the central and peripheral nervous system as competitive, non-selective muscarinic acetylcholine receptor (mAChR) antagonists, which prevent binding of the physiological neurotransmitter acetylcholine. The agonist properties of hyoscyamine and scopolamine give rise to several important pharmacological effects, such as antispasmodic actions on the gastrointestinal tract and antisecretory effects controlling salivary secretions during surgical operations [1] [2]. Atropine, (a mixture of both L-(2*'S*) and D-(2*'R*) enantiomers of hyoscyamine) is used as an antidote against cholinesterase inhibitors poisoning and also for dilating the pupil of the eye during eye examinations. The market demand for hyoscyamine and scopolamine is increasing and the chemical synthesis of these alkaloids has proved to be difficult and commercially infeasible. In addition, the commercial demand for scopolamine is estimated to be tenfold higher than for hyoscyamine due to its fewer adverse effects and higher physiological activity [3].

1.2. Hyoscyamine 6β-Hydroxylase Is a 2-Oxoglutarate-Dependent Dioxygenase (2OGD)

The conversion of hyoscyamine into scopolamine is catalyzed by hyoscyamine 6β-hydroxylase (EC 1.14.11.11, H6H), a key enzyme catalyzing the hydroxylation of L-hyoscyamine to 6β-hydroxyhyoscyamine (anisodamine) and its subsequent epoxidation to scopolamine (**Figure 1**) [4]. H6H is considered an important key enzyme in the biosynthetic pathway for scopolamine and its gene has been isolated from various scopolamine-producing species [5]. Several studies were performed in attempts to enhance scopolamine accumulation in plants by the overexpressing *H6H* gene [6] [7] [8] [9]. Hashimoto and Yamada (1986) [10] showed that the hyoscyamine 6β-hydroxylase from *Hyoscyamus niger* preferentially accepted the L-(2*'S*) isomer of hyoscyamine as a substrate and that the D-(2*'R*) isomer of hyoscyamine was nearly inactive. This was further corroborated in the recombinant *MaH6H* from *Mandragora autumnalis* [11] that encodes an active H6H enzyme. Still, a possible mechanism for this enantiomeric preference was not explained. Moreover, Schlesinger *et al.* (2019) [11] showed that a substitution of the Gly-220 residue for a cysteine was linked to the lack of

scopolamine and anisodamine phenotypes in *M. officinarum* accessions. Although *M. officinarum* accessions displayed a functionally inactive H6H, and this amino acid substitution was strongly linked with the alkaloid composition phenotype as determined by cleaved amplified polymorphic sequences (CAPS) analysis, the direct influence on the functionality of the specific Gly-220 substitution as related to other amino acid changes in the H6H protein was not tested. Recently Kluza *et al.* (2020) [12] published a high-resolution crystal structure of the *D. metel* H6H and shed light on the molecular basis of H6H specificity towards hyoscyamine. The authors mentioned the possibility that a Gly220Cys substitution may disturb hyoscyamine binding through re-arrangement of the hydrophobic cavity of the protein, but the exact mechanism of this interference remained to be shown. Because of the proximity of Gly-220 to the phenyl ring of hyoscyamine during catalysis and the high level of sequence conservation in H6H proteins, we hypothesized that a deliberate substitution of the Gly-220 to a Cys residue could render an enzymatically inactive protein. Using protein modeling, we delineate here the apparent role of Gly-220 in the binding capacity of the H6H protein and the disruption caused when it was replaced with cysteine. In addition, our model provides a biochemical rationale for the enantiomeric preference of DiH6H for the L-(2*'S*)-isomer of hyoscyamine.

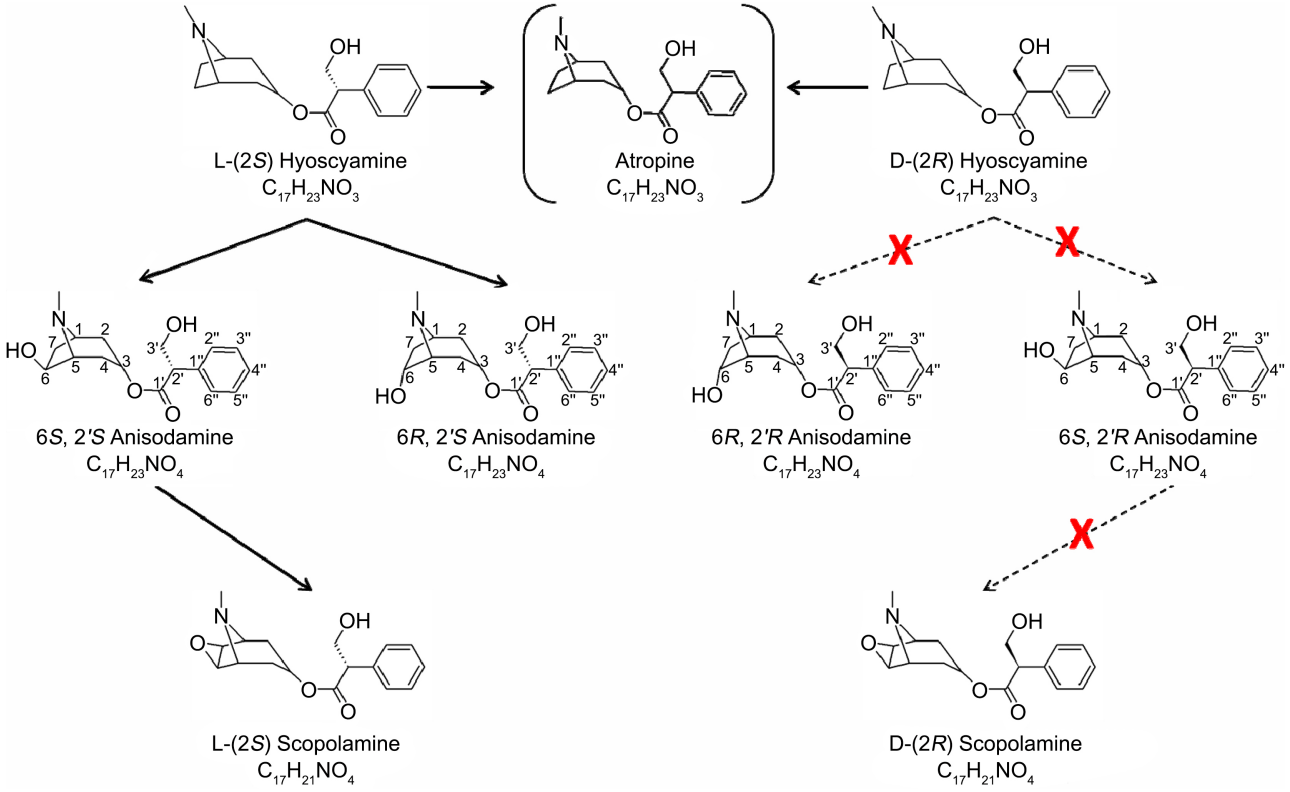

Figure 1. The sequential conversion of hyoscyamine into anisodamine and scopolamine by the action of hyoscyamine 6*β*-hydroxylase (H6H). Atropine is a racemic mixture of L-(2*'S*) and D-(2*'R*) hyoscyamine, but only L-(2*'S*) hyoscyamine is present in plants and is hydroxylated to anisodamine (6*β*-hydroxyhyoscyamine) that in turn is epoxidated to (2*'S*)-scopolamine. Red X designate inefficient biochemical processes. The carbon numbering system for each compound is according to [11].

2. Material and Methods

2.1. Plant Material

Seeds of *D. innoxia* were collected in the Beit She'arim area, Jezre'el Valley, Israel. After germination, the plants were grown in pots in a net-house located at Newe Yaar Research Center in Israel and were irrigated daily during the morning.

2.2. RNA Extraction, Sequencing and Transcriptome Assembly

Leaves and roots of *D. innoxia* were sampled from a mature, 2-months old, flowering plant. The tissues were frozen in liquid N_2 and ground into a uniform powder using a chilled mortar and pestle. RNA was extracted using the SIGMA Plant total RNA kit following the manufacturer's protocol. Total RNA was used for Mrna seq library construction and Illumina sequencing. RNA sequencing was performed according to Schlesinger *et al.* (2019) [11].

2.3 Assembly and Candidates Search

Reads were assembled *de novo* using Trinity software (version: v2.3.2; [13] with the trimmomatic option to remove adaptors [14] and 25 mer k-mer size. A tBLASTn search using the *H*yoscyamus *niger HnH6H* (**AAA33387.1**) [4] was performed on the newly acquired transcriptome of *D. innoxia*. The candidate gene identified was identical to the previously reported *D. innoxia* DiH6H (**MH392211**) [15].

2.4. Isolation and Synthesis of DiH6H and DiH6H_G_{220}C

For the isolation of the *DiH6H* candidate gene, cDNA was synthesized from 0.2 μg of total RNA using the Verso cDNA synthesis kit (Thermo Fisher scientific, Kiryat Shmona, Israel). The amplification was done with specific primers designed for cloning into pET-28a according to the transcriptomic sequence results of the BLAST search. The primers employed were as follows: 5'-AAGCTA GCATGGCTACTCTTGTCTCAAATTGGT-3' and 5'-TTCTCGAGTTAATTAG GGAATTGATTGATTTTATATGGTTTAACACC-3'. The amplification of the *DiH6H* gene was done using 120 ng of the cDNA and the Phusion high-fidelity PCR master mix (Thermo Fisher scientific, Kiryat Shmona, Israel). The conditions of the PCR were according to the T*m* of the primers and to the Phusion high-fidelity PCR master mix protocol. *DiH6H_G_{220}C* was synthesized and obtained from Twist Bioscience (South San Francisco, CA). Both *DiH6H* and *DiH6H_G_{220}C* genes were ligated into pET-28a plasmid using *XhoI* and *NheI* (New England Biolabs) restriction enzymes and transformed into *Escherichia coli* (*E. coli*) DH5α for plasmid purification and sequencing. For sequencing, the *DiH6H* and *DiH6H_G_{220}C* were amplified using the T7 terminator and T7 promotor primers and sequenced (Sanger) with an Applied Biosystems 3130xl Genetic Analyzer (Applied Biosystems, http://www.appliedbiosystems.com) according to the manufacturer's instructions.

2.5. Functional Expression Analyses

The procedure was essentially as described in [11]. In brief, the plasmids containing each gene were introduced to the expression strain *E. coli* BL21 (DE3). A fresh bacterial culture harboring the recombinant plasmid was grown in 5 ml of Luria-Bertani (LB) liquid medium until it reached an OD_{600} between 0.6 and 0.8. IPTG (1mM final concentration) was added for induction of the ectopically expressed gene. Atropine or anisodamine were added to the medium as substrates to a final concentration of 0.35 mM.

2.6. LC-Q-TOF-MS/MS Analysis

For functional expression analysis experiments, 1 ml of the bacterial cultures were centrifuged in an Eppendorf tube at 14,000 g for 5 min and filtered through a 13 mm Syringe filter with 0.2 μm GH Polypro membrane (Acrodisc) into a 2 ml vial for further analysis in LC-Q-TOF-MS/MS. The analyses were carried out on an Agilent 1290 Infinity series liquid chromatograph coupled with an Agilent 6530 Accurate Mass Quadrupole Time-of-Flight (Q-TOF) LC/MS equipped with the Agilent Jet Stream interphase (Agilent Technologies, Santa Clara, USA). The analytical column was a Zorbax Extend-C18 Rapid Resolution HT column (2.1 × 50.0 mm, 1.8 μm, Agilent Technologies, Waldbronn, Germany). The conditions were as in Schlesinger *et al.* (2019) [11].

2.7. Modeling

Structure models of the two DiH6H variants (Gly-220 and Gly220Cys) were constructed using SWISS-MODEL [16]. The model processing was performed based on the tH6H 1.12A crystal structure of *D. metel* (PDB code: 6ttn) (98% identity), which includes hyoscyamine and N-oxalylglycine as substrates and Ni(II) as a cofactor. The substrates, hyoscyamine and oxalylglycine (an inactive co-substrate analog to 2-oxoglutarate, 2OG) were utilized for the modeling process of the intact DiH6H. Regarding the DiH6H_G_{220}C structure, a hyoscyamine molecule was docked into the protein using AutoDock Vina [17]. The position of the docked hyoscyamine molecule was identical to the crystal structure (PDB code. 6ttm). Schematic diagram of protein-ligand interaction was assembled using the LIGPLOT program [18]. Structural analysis and visualization were performed using the PyMOL software package [19]. The role of the hydroxyl group on carbon 3 'was found in the DmH6H structure (PDB: 6ttn), analyzed in the protein data bank (PDB) site.

3. Results

3.1. Identification of *DiH6H*, a Hyoscyamine 6*β* Hydroxylase from *Datura innoxia*

The nucleotide sequence of *DiH6H* (MH392211) [15] was not available, therefore we searched our root and leaf transcriptome using the functionally active *H. niger* H6H (HnH6H) (AAA33387.1) gene [4] as a template. A tBLASTn search

revealed a highly similar sequence (1044 bp) encoding a protein (347 a.a) displaying 100% nucleotide sequence identity to the DiH6H (MH392211) [15] leaf. Transcript abundance analysis, as measured by fragments per kilobase of transcript per million fragments in our Illumina database, indicated that *DiH6H* is preferentially expressed in root tissues (155 fpkm), with undetectable expression levels in the leaf.

3.2. The Biochemical Functionality of DiH6H

In order to verify the biochemical functionality of DiH6H and DiH6H_G_{220}C, enzyme assays using atropine (a racemic mixture of hyoscyamine enantiomers) and anisodamine (a mixture of 2 enantiomeric pair isomers) as substrates were conducted. Each of the substrates was added to *E. coli* cultures, ectopically expressing *DiH6H* or *DiH6H_G_{220}C*. The presence of anisodamine and scopolamine in the growth medium was tested using LC-Q-TOF-MS/MS. When atropine was added as a substrate, the media, supporting *E. coli* expressing DiH6H, contained scopolamine eluting at 2.43 min and exhibiting *m*/*z* [M + H] of 304.1548 (**Figure 2(a_1)**). Additionally, two peaks with *m*/*z* [M + H] of 306.1700, corresponding to stereoisomers of anisodamine, were noted (**Figure 2(a_1)**). The first peak, eluting at 1.87 min, was assigned as 6*R*, 2*'S* anisodamine and the second peak, eluting at 3.4 min, assigned as 6*S*, 2*'S* anisodamine. Our assignment of the two enantiomeric pairs of anisodamine was based on Wu *et al.* (2019) [20] that separated the diastereomeric and enantiomeric anisodamine isomers using high-performance liquid chromatography (HPLC). When anisodamine was added as a substrate to the growth medium harboring DiH6H, scopolamine was produced (**Figure 2(b_1)**). The retention time of the anisodamine isomers and scopolamine products corresponded to the authentic standards, respectively (**Figure 2(c)**). To attain a more rigorous identification of the products released to the bacterial media, we used tandem mass spectrometry for each compound. The fragmentation of each compound indicated the presence of scopolamine and anisodamine (**Figure 3**). The two anisodamine isomers show the same fragmentation pattern but displayed only minor different ratios between them that did not allow for their specific stereoisomeric identification based on mass spectroscopy.

3.3. The Influence of Gly220Cys Substitution on the Biochemical Functionality of DiH6H

In order to assess the influence of the Gly220Cys substitution on the protein enzymatic functionality, an enzyme assay using the recombinant DiH6H_G_{220}C was performed. In contrast to DiH6H, the media supporting *E. coli* cultures expressing the DiH6H_G_{220}C to which atropine was added were devoid of either scopolamine and anisodamine (**Figure 2(a_2)**). In addition, when synthetic anisodamine, which includes four isomers of anisodamine (**Figure 1**), was administered as a substrate to the cultures, scopolamine was absent in the media (**Figure 2(b_2)**).

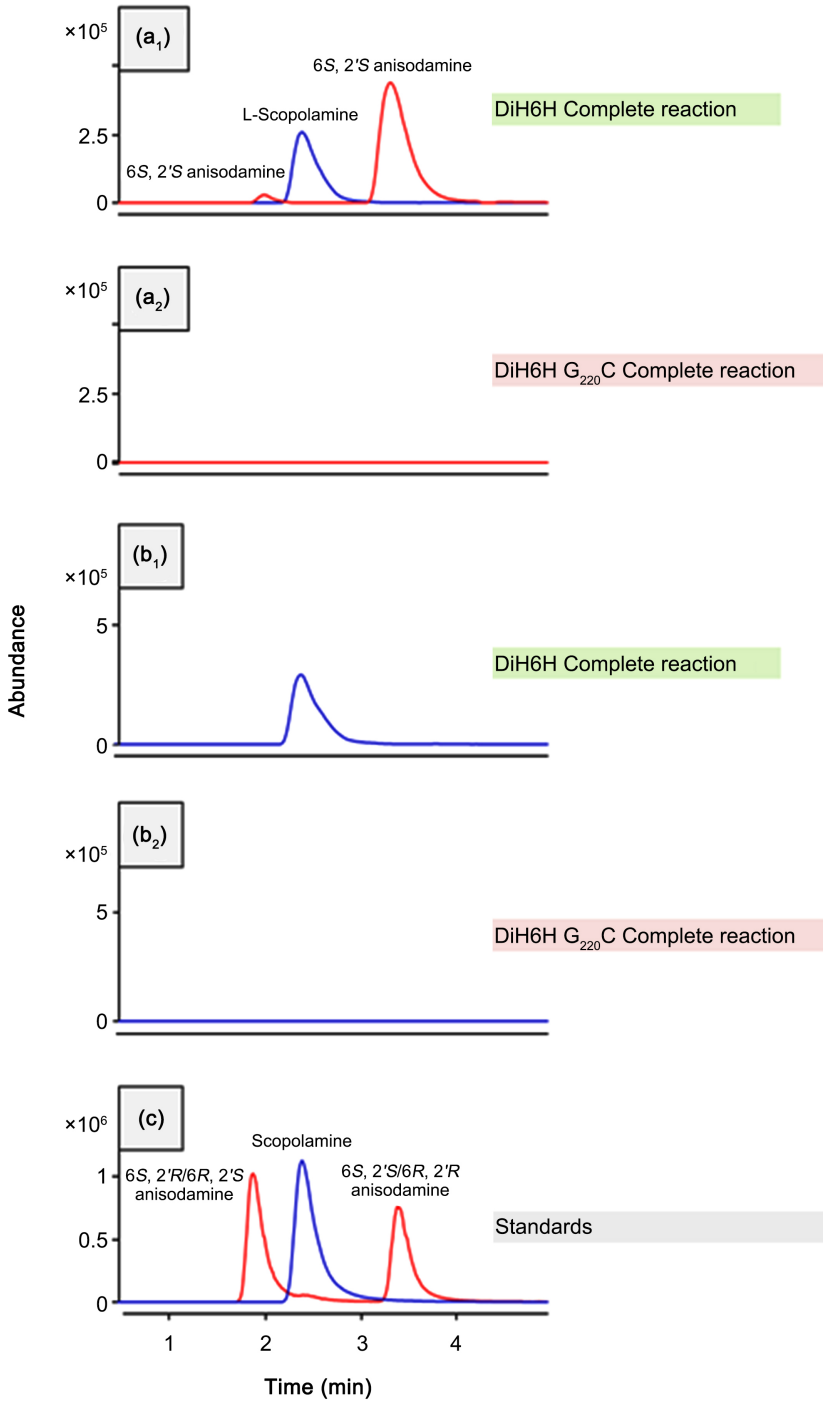

Figure 2. Functional expression of DiH6H and DiH6H_G$_{220}$C in *E. coli.* Extracted ion chromatograms of scopolamine (*m/z* [M + H] 304.1548) and anisodamine isomers (*m/z* [M + H) 306.17) in the culture medium of *E. coli* expressing the respective H6H gene and supplemented with atropine (a) or anisodamine isomers (b) as substrates. The products were identified by comparison of their R*t* with authentic standards (c) and by their mass spectra (**Figure 3**). The recombinant DiH6H causes a release of scopolamine to the bacterial medium when atropine (a_1) or anisodamine (b_1) are added as substrates, while the addition of anisodamine isomers results in the accumulation of scopolamine (b_1). DiH6H losses both its hydroxylating functionality (a_2) and epoxidating functionality (b_2) when the Gly-220 residue is replaced with a Cys-220.

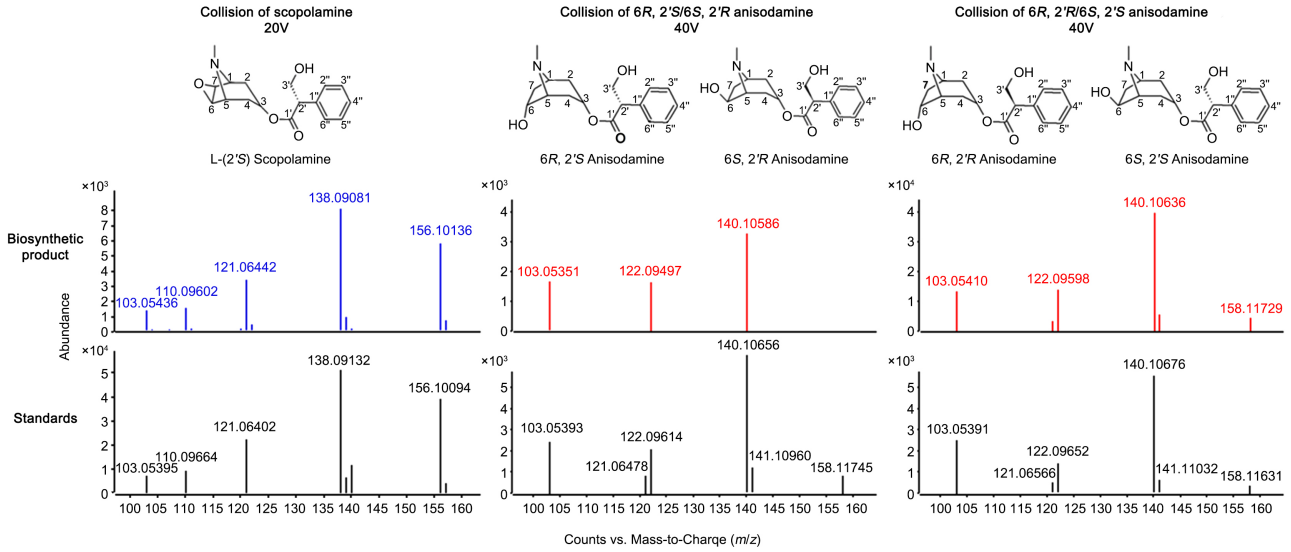

Figure 3. The identification of scopolamine and anisodamine isomers generated by DiH6H by tandem mass – spectrometry. Top panels indicate biosynthetic products and bottom panels indicate the mass spectra of authentic standards.

3.4. The Role of Gly-220 in Forming the Hydrophobic Cavity of DiH6H

To better understand the influence of the Gly220Cys substitution on DiH6H activity, we checked the role of Gly-220 residue in the protein structure; thus, the original protein (exhibiting Gly-220) was modeled using the SWISS-MODEL server [16]. The examination of the model clearly demonstrated the high structural complementary topographies between hyoscyamine and the protein binding pocket, mainly where the phenyl-ring is anchored (**Figure 4(a)**). Furthermore, when looking at the area where the Gly-220 resides (**Figure 4(b)**), is it highly noticeable that the Gly-220 surface exactly fits with the hyoscyamine phenyl ring surface and directly participates in creating the cavity around the phenyl ring of hyoscyamine. It seems that the cavity surrounding the phenyl ring acts as an anchor for either hyoscyamine or anisodamine, stabilizing the substrates for both the hydroxylation and epoxidation reactions that occur on the other side of the hyoscyamine molecule. The structure model was then analyzed using LIGPLOT, a program that generates schematic diagrams of protein-ligand interactions [18]. LIGPLOT analysis (**Figure 5**) indicates that chief interactions of hyoscyamine with the surrounding pocket are hydrophobic, especially in the area where the phenyl ring is anchored. The surrounding hydrophobic and non-polar amino acids are Phe-103, Leu-107, Met-196, Leu-198, Asn-221, Leu-290, Tyr-319, Ala-323, Tyr-326, Leu-327, and the Gly-220.

3.5. The Interference of the Gly220Cys Substitution on the DiH6H Structure

For a deeper understanding of the influence of the Gly220Cys substitution on DiH6H structure, the DiH6H_G_{220}C protein was modeled, also using the SWISS-MODEL server. The model of the original Gly-220 DiH6H protein in-

cluded the substrates, hyoscyamine, oxalylglycine and the iron cofactor in the crystal structure while the mutant, DiH6H_G_{220}C, displayed only the oxalylglycine and the iron cofactor but hyoscyamine was not displayed (**Figure 6**). This modeling demonstrates the involvement and importance of Gly-220 in the binding of L-hyoscyamine. Conversely, when examining the model corresponding to the mutant DiH6H_G_{220}C, we found that the Cys-220 surface clashes and interferes in a non-chemical manner with the phenyl surface of hyoscyamine (**Figure 4(c)**).

3.6. The Role of the Hydroxyl Group on Carbon 3'

The enantiomeric preference of the H6H protein for the L-2*'S* isomer of hyoscyamine was noted by Hashimoto and Yamada (1986) [10], but a biochemical rationale for this preference was not elaborated. Interestingly, when examining the DmH6H crystal structure binding site, we noted that the hydroxyl group on carbon 3*'* of L-hyoscyamine interacts with Tyr-295 and Leu-290 through two crystallographic water molecules (H_2O 689 and 843) (**Figure 7**). Surprisingly when docking the two enantiomers of hyoscyamine into the original model of DiH6H, the results did not show steric clashes or cavity fitness drawbacks.

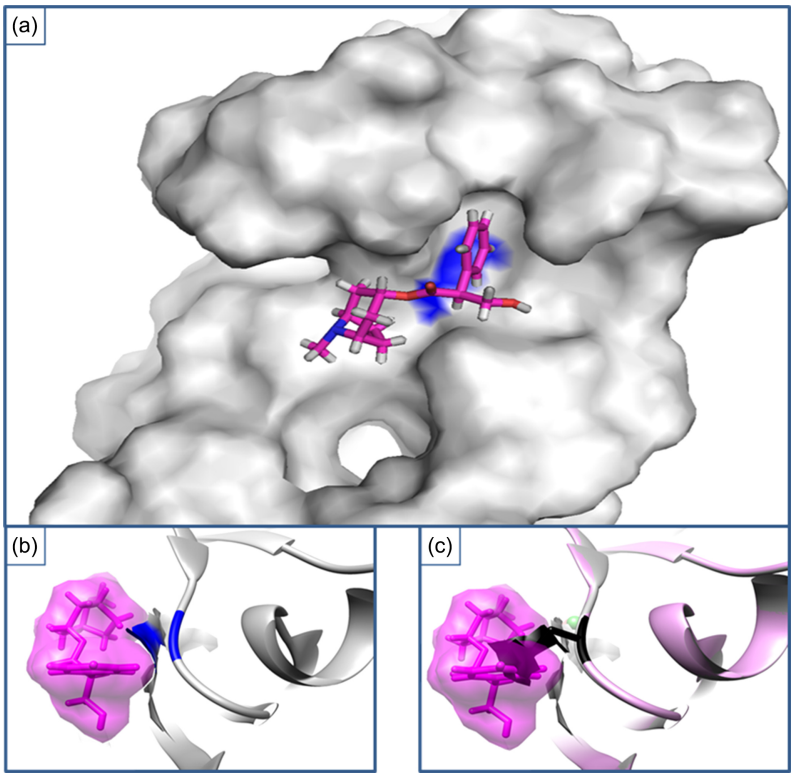

Figure 4. DiH6H modeling showing the pocket where anisodamine and hyoscyamine reside and the effect of Gly220Cys substitution on hyoscyamine electronic surface. (a) Surface presentation emphasizing the shape of the hyoscyamine binding site. The Gly-220 surface, which participates in creating the binding cavity is shown in blue. (b) Surfaces fitness of Gly-220 (Blue) and hyoscyamine phenyl-ring (pink surface). (c) The clash between the Cys-220 surface (black) to the hyoscyamine phenyl ring surface (pink).

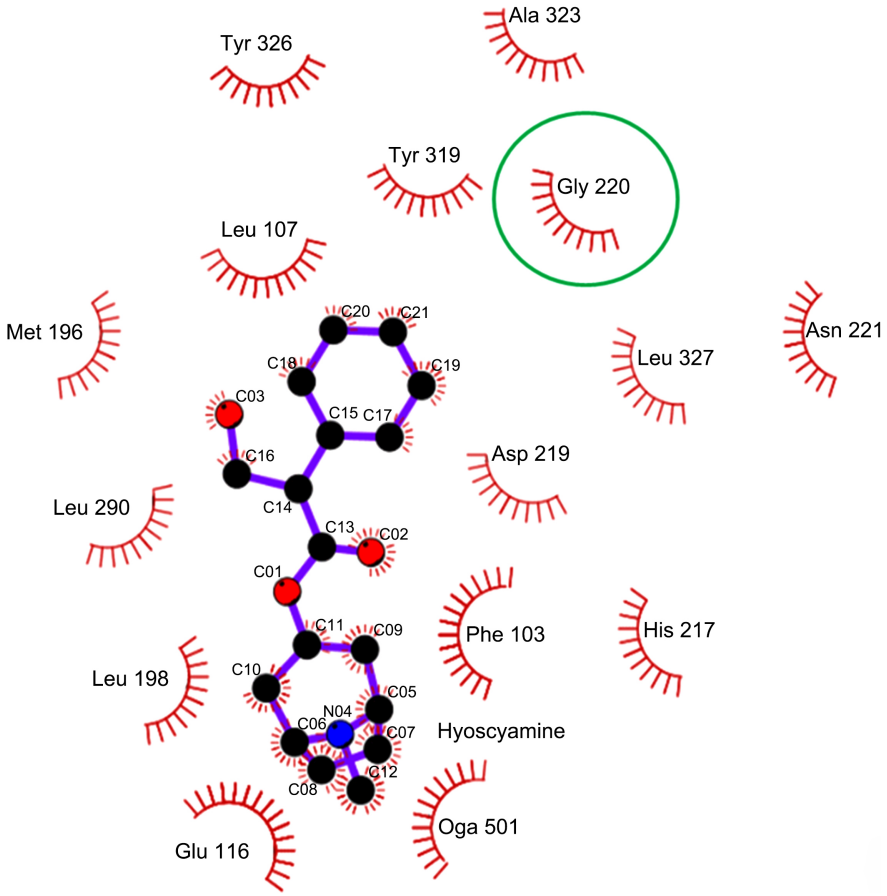

Figure 5. LIGPLOT schematic diagram showing the amino acids that are responsible for creating the cavity in H6H where hyoscyamine and anisodamine reside. Non-polar and hydrophobic amino acids, create hydrophobic interactions (shown as red arches) with hyoscyamine. Among them is the Gly-220 (in green circle), indicating its essential role in forming the catalytic hydrophobic cavity around the phenyl ring of L-Hyoscyamine. Oga-N-oxalylglycine.

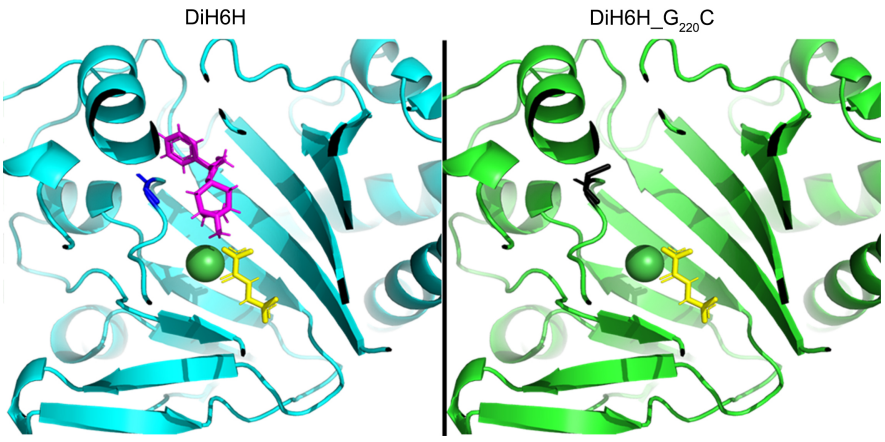

Figure 6. Protein models of DiH6H (left) and DiH6H_G_{220}Cys (right) generated by the SWISS-MODEL server. In DiH6H, where Gly-220 is present (blue), hyoscyamine (pink), oxalylglycine (yellow) and Fe^{2+} (green) are correctly localized. In contrast, in the DiH6H_G_{220}Cys model, where Cys-220 (Black) is present, only oxalylglycine and Fe^{2+} were localized, while hyoscyamine could not fit the model under these conditions.

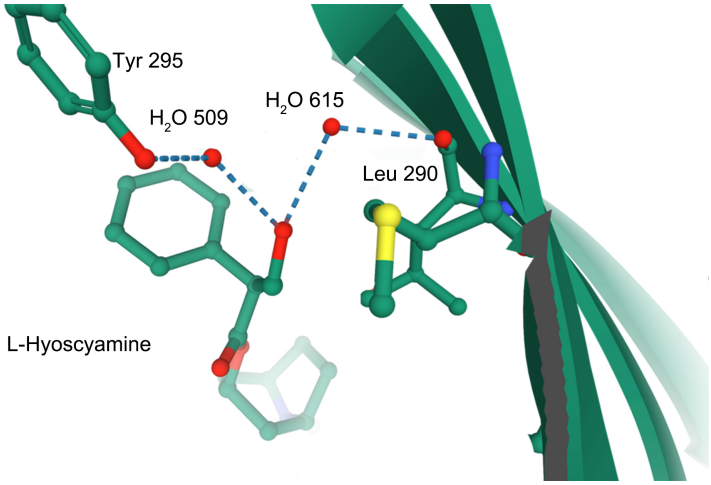

Figure 7. The role of hydrogen bonding of the 3' hydroxyl group of hyoscyamine and anisodamine in stabilizing the active pocket of H6H. The DmH6H structure (PDB 6ttn) indicates a clear interaction of the 3' hydroxyl group with Tyr-295 and Leu-290 through two crystallographic water molecules (H_2O 689 and 843). Green, red, yellow and blue represent carbon, oxygen, sulfur and nitrogen atoms, respectively. The dashed blue line represents hydrogen bonds.

4. Discussion

4.1. The Functionality of DiH6H and the Formation of an Additional Anisodamine Isomer

The ability of H6H protein to generate scopolamine from L-hyoscyamine and anisodamine has been demonstrated in several Solanaceae species, including *H. niger*, *A. tanguticus*, *A. acutangulus*, *A. belladonna*, *Brugmansia sanguinea*, *M. autumnalis*, *D. metel* [5] [11] [16] [21] [22] [23] [24] [25] and recently also in *D. innoxia* [17]. This gene was previously functionally expressed and the isolated protein was shown to accept L-hyoscyamine and anisodamine as substrates [15]. Our studies further indicate that *E. coli* cultures overexpressing DiH6H accept atropine, forming anisodamine and scopolamine (**Figure 2(a_1)**), as well as anisodamine, forming scopolamine (**Figure 2(b_1)**) and the products are released into the bacterial growth medium. Moreover, when atropine (a racemic mixture of L-(2*'S*) and D-(2*'R*) hyoscyamine) was added to *E. coli* cultures harboring DiH6H, two peaks, at 1.87 and 3.4 min, were detected (**Figure 2(a_1)**). The two peaks correspond to the two isomers of anisodamine. The large peak, eluting at 3.4 min, represents the 6*S*, 2*'S* isomer of anisodamine that later is epoxidized into scopolamine. The low abundance peak eluting at 1.87 min represents the 6*R*, 2*'S* isomer of anisodamine that cannot be epoxidated into scopolamine due to the hydroxyl group on carbon 6 being in the opposite direction. Our assignment for each peak was based on the studies of Wu *et al.* (2019) [20] that separated the four isomers of synthetic anisodamine by HPLC. In addition, using tandem mass-spectrometry, we were able to validate the chemical identification of all substances by their identical fragmentation pattern as compared to authentic standards (**Figure 3**). Although the 6*S*, 2*'S* and 6*S*, 2*'R* isomers of anisodamine

displayed different fragmentation ratios, the differences were minor and we were not able to distinguish between them using tandem mass-spectrometry under our conditions (**Figure 3**). The ability of DiH6H to form an additional anisodamine isomer from atropine was not reported by Li *et al.* (2020) [15]. Our results further indicate the production of both the 6*'S* and 6*'R* isomers of anisodamine by the H6H enzyme and its preference for the 6*'S* stereoisomeric form of its substrates. Corroborating earlier studies by Hashimoto and Yamada, (1986) [10] that indicated that the *H. niger* H6H exclusively accepts L-(2*'S*)-hyoscyamine as a substrate and hydroxylates it in a (6*S*) position.

4.2. The Importance of the Gly220 Residue for Catalysis

Similarly to all active H6H enzymes known in the Solanaceae, DiH6H displays an amino acid glycine at residue 220. This Gly-220 is located close to the Asp219 amino acid that is part of the highly conserved $HXDX_nH$ triad motif prevalent among members of the 2OGD family. This motif includes three highly invariant and conserved residues that are essential for Fe(II) binding [26]. The Gly-220 appears in all the functional active H6Hs (**Figure 8**). Accordingly, in the biochemically inactive MoH6H, from *M. officinarum*, a natural modification of Gly-220 for a cysteine was prominent. MoH6H was not functional, and the Gly/Cys substitution was related to the inability to produce scopolamine in naturally grown accessions of *M. officinarum* that accumulated significant levels of hyoscyamine but contained neither anisodamine nor scopolamine [11]. Interestingly, when the Gly-220 in DiH6H was replaced with Cys-220 (as found in the non-functional MoH6H), DiH6H lost its ability to perform the hydroxylation of hyoscyamine to anisodamine (**Figure 2(a_2)**) and the epoxidation of anisodamine to scopolamine (**Figure 2(b_2)**). Our results provide biochemical evidence for our previous hypothesis that the Gly220Cys substitution found in MoH6H could be attributed to its loss of function and the alkaloid chemodiversity in *Mandragora* spp. [11].

4.3. The role of Gly-220 in Hyoscyamine 6*β* Hydroxylase Activity and the Effect of Its Substitution with Cysteine

The quasi-perfect match between the DiH6H protein and its substrate hyoscyamine is highly prominent in our model, especially around the area where the phenyl ring of hyoscyamine is present (**Figure 4(a)**). The role of Gly-220 residue in this interaction is also apparent when examining the surfaces of both Gly-220 and hyoscyamine. The surface of Gly-220 residue wraps the surface of the phenyl ring with minimal electronic interaction (**Figure 4(b)**). It seems plausible that the cavity formed by Gly-220 and the residues surrounding it acts as an anchor for the phenyl ring of hyoscyamine and anisodamine, allowing the hydroxylation and epoxidation to occur on the other side of the molecule. Conversely, in the DiH6H_G_{220}C model, the influence of Gly220Cys substitution on the protein structure and consequently, on its catalytic activity, is clearly noticeable. When

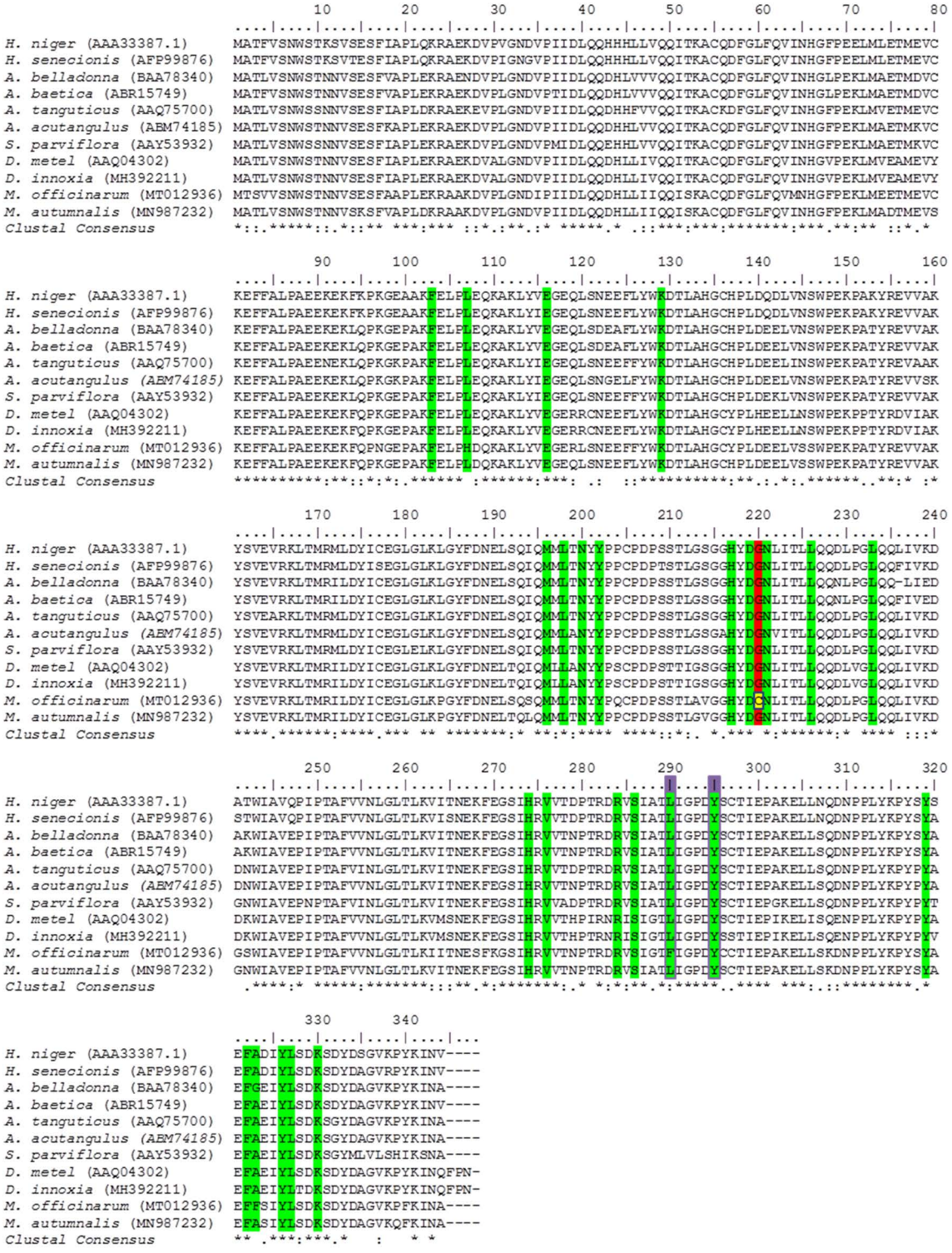

Figure 8. Comparison of amino acid sequences showing the catalytic amino acids in functionally characterized H6H sequences from Solanaceae species. Conserved residues found to have key roles in H6H catalytic activity are marked in green. The Gly-220 marked in red is conserved in all species except for the catalytically inactive MoH6H from *M. officinarum* that contains Cys-220 (marked in yellow in a blue square). The surrounding hydrophobic and non-polar amino acids that take part in forming the catalytic cavity are Phe-103, Leu-107, Met-196, Leu-198, Asn-221, Leu-290, Tyr-319, Ala-323, Tyr-326, Leu-327, and the Gly-220. Leu-290 and Tyr-295 (marked in a purple square) stabilize the 3' beta hydroxyl group of the substrate with hydrogen bonding through two crystallographic water molecules.

cysteine resided in residue 220, its thiol side-chain surface penetrates the phenyl ring surface and blocks the cavity where the phenyl ring of hyoscyamine and anisodamine are normally docked (**Figure 4(c)**). In order to have a deeper understanding of the Gly-220 role in the DiH6H protein pocket, we used the LIGPLOT program to find the protein-ligand interactions present in the DiH6H protein. In **Figure 5**, we show 14 residues that exert hydrophobic interactions with hyoscyamine and create the cavity where the substrate resides in the protein. Among these residues, Gly-220 is prominent and constitutes one of several hydrophobic, non-polar amino acids that are crucial for the protein hydrophobic interactions with the phenyl rings of hyoscyamine and anisodamine (**Figure 6**). When the hydrophobic Gly-220 is replaced with a polar amino acid such as cysteine, the hydrophobic interaction with the phenyl ring is prevented and the hydrophobic cavity is largely disrupted.

4.4. The 2*'S* Position of the Hydroxyl Group in Hyoscyamine and Anisodamine Is Crucial for Proper Protein Binding

The preference of H6H for the L-(2*'S*)-isomer of hyoscyamine was demonstrated by Hashimoto and Yamada (1986) [10] using a H6H protein from *H. niger* that formed anisodamine only when the 2*'S* isomer of hyoscyamine was given, and essentially did not accept the 2*'R* isomer of hyoscyamine. A rationale for this isomeric preference was not given. The crystallographic structure reported by Kluza *et al.* (2020) [12] enabled us to check the role of the hydroxyl group bound to the 3*'* carbon (**Figure 1**). Our results, depicted in **Figure 7**, show that this hydroxyl group creates hydrogen bonds with Tyr-295 and Leu-290 through two crystallographic water molecules (689 and 843). Since the alcohol on carbon 3*'* faces the opposite direction in the D-(2*'R*)-isomer of hyoscyamine, we assume that these hydrogen bonds cannot be formed and the stability of hyoscyamine in the active site is compromised. Tyr-295 and Leu-290 are conserved residues in all H6H (**Figure 8**). Therefore these observations likely apply for the rationalization of the enantiomeric specificity of H6H enzymes.

4.5. The Amino Acids Involved in Substrate and Co-Substrate Binding, and in Forming the Catalytic Cavity, Are Highly Conserved among H6H's

Until the recently published crystal structure of DmH6H was available [12], the only recognized conserved regions regarding H6H were the conserved iron-binding sites and the conserved $HXDX_nH$ catalytic site related to the 2OGD family [4] [27] [28]. In the present study, we show amino acids sequence alignment of functionally tested H6H's from scopolamine producing Solanaceae (**Figure 8**). The specific amino acids involved in forming the substrate binding pocket, exert a direct interaction with hyoscyamine are marked in green. In detail, the conserved amino acids include:

- The Gly-220 that, according to our results from the LIGPLOT server (**Figure 5**), takes part in forming the hydrophobic cavity for hyoscyamine together

with Phe-103, Leu-107, Met-196, Leu-198, Asn-221, Leu-290, Tyr-319, Ala-323, Tyr-326, Leu-327 [18].

- The $H_{217}XD_{219}X_{220\text{-}273}H_{274}$ ("facial triad") that forms a metal binding motif and is highly conserved in the OGD family [27] [29].
- The hydrophobic residues Leu-226, Leu-233 and Val-276 that line the co-substrate binding pocket along with Asn-200, Tyr-202, Arg-284 and Ser-286 that form hydrogen bonds with 2OG.
- The Phe-103, Tyr-295, Tyr-319, Phe-322 and Tyr-326 which form the aromatic cage, where the phenyl ring of hyoscyamine is bound.
- The amino acid that stabilizes the tropane ring by hydrophobic interactions (Leu-198 and Leu-290), hydrogen bond (Phe-103) and electrostatic interaction between Glu-116 and the tertiary amine group.
- Lys-129 and Lys-330 that stabilize the arrangement of Glu-116 and hyoscyamine.

All the above-mentioned residues are highly conserved and appear in all H6H's proteins from different Solanaceae species. The only exceptions are Leu-107 and Leu-290 that are replaced by phenylalanine and histidine, respectively and the Gly-220 (marked in red) that is replaced by Cys-220 (marked in yellow) in the functionally inactive *M. officinarum* MoH6H.

5. Conclusion

The commercial demand for scopolamine is estimated to be tenfold higher than for hyoscyamine due to its fewer adverse effects and higher physiological activity [3]. Our results shed light on the importance of the Gly220 residue found in all H6H proteins present in scopolamine producing species. Using molecular modeling, we indicate a possible mechanism by which the Gly220Cys substitution disrupts substrate binding and interferes with catalysis. We also provide a biochemical rationale for the enantiomeric preference of DiH6H for the L-(2*'S*) hyoscyamine. Our observations could be funneled for the industrial efforts to produce scopolamine using biotechnological tools.

Acknowledgements

The research leading to these results has received funding from the European Union's Seventh Framework Programme for research, technological development and demonstration under grant agreement n˚ 613513. The authors thank Federica Cattonaro and Vera Vendramin for the Illumina sequencing. We also thank Shimon Ben Shabat for useful discussions.

Conflicts of Interest

The authors declare no conflicts of interest regarding the publication of this paper.

References

[1] Dewick, P.M. (2002) Alkaloids. In: *Medicinal Natural Products: A Biosynthetic Ap-*

proach, 2nd Edition, John Wiley & Sons, London, 292-302.

[2] Elrod, K. and Buccafusco, J.J. (1988) An Evaluation of the Mechanism of Scopolamine-Induced Impairment in Two Passive Avoidance Protocols. *Pharmacology, Biochemistry and Behavior*, **29**, 15-21. https://doi.org/10.1016/0091-3057(88)90267-5

[3] Ullrich, S.F., Hagels, H. and Kayser, O. (2017) Scopolamine: A Journey from the Field to Clinics. *Phytochemistry Reviews*, **16**, 333-353. https://doi.org/10.1007/s11101-016-9477-x

[4] Matsuda, J., Okabe, S., Hashimoto, T. and Yamada, Y. (1991) Molecular Cloning of Hyoscyamine 6β-Hydroxylase, a 2-Oxoglutarate-Dependent Dioxygenase, from Cultured Roots of *Hyoscyamus niger*. *Journal of Biological Chemistry*, **266**, 9460-9464. https://doi.org/10.1016/S0021-9258(18)92843-7

[5] Kai, G., Liu, Y., Wang, X., Yang, S., Fu, X., Luo, X. and Liao, P. (2011) Functional Identification of Hyoscyamine 6β-Hydroxylase from *Anisodus acutangulus* and Overproduction of Scopolamine in Genetically-Engineered *Escherichia coli*. *Biotechnology Letters*, **33**, 1361-1365. https://doi.org/10.1007/s10529-011-0575-y

[6] Wang, X., Chen, M., Yang, C., Liu, X., Zhang, L., Lan, X., Tang, K. and Liao, Z. (2011) Enhancing the Scopolamine Production in Transgenic Plants of *Atropa belladonna* by Overexpressing *Pmt* and *H6h* Genes. *Physiologia Plantarum*, **143**, 309-315. https://doi.org/10.1111/j.1399-3054.2011.01506.x

[7] Kang, Y.M., Park, D.J., Min, J.Y., Song, H.J., Jeong, M.J., Kim, Y.D., Kang, S.M., Karigar, C.S. and Choi, M.S. (2011) Enhanced Production of Tropane Alkaloids in Transgenic *Scopolia parviflora* Hairy Root Cultures Over-Expressing Putrescine N-Methyl Transferase (PMT) and Hyoscyamine-6beta-Hydroxylase (H6H). *In Vitro Cellular and Developmental Biology—Plant*, **47**, 516-524. https://doi.org/10.1007/s11627-011-9367-2

[8] Yang, C., Chen, M., Zeng, L., Zhang, L., Liu, X., Lan, X., Tang, K. and Liao, Z. (2011) Improvement of Tropane Alkaloids Production in Hairy Root Cultures of *Atropa belladonna* by Overexpressing *Pmt* and *H6h* Genes. *Plant OMICS Journal*, **4**, 29-33. https://doi.org/10.1111/j.1399-3054.2011.01506.x

[9] Kai, G., Zhang, A., Guo, Y., Li, L., Cui, L., Luo, X., Liu, C. and Xiao, J. (2012) Enhancing the Production of Tropane Alkaloids in Transgenic Anisodus Acutangulus Hairy Root Cultures by Over-Expressing Tropinone Reductase i and Hyoscyamine-6β-Hydroxylase. *Molecular BioSystems*, **8**, 2883-2890. https://doi.org/10.1039/c2mb25208b

[10] Hashimoto, T. and Yamada, Y. (1986) Hyoscyamine 6β-Hydroxylase, a 2-Oxoglutarate-Dependent Dioxygenase, in Alkaloid-Producing Root Cultures. *Plant Physiology*, **81**, 619-625. https://doi.org/10.1104/pp.81.2.619

[11] Schlesinger, D., Davidovich Rikanati, R., Volis, S., Faigenboim, A., Vendramin, V., Cattonaro, F., Hooper, M., Oren, E., Taylor, M., Sitrit, Y., Inbar, M. and Lewinsohn, E. (2019) Alkaloid Chemodiversity in *Mandragora* Spp. Is Associated with Loss-of-Functionality of MoH6H, a Hyoscyamine 6β-Hydroxylase Gene. *Plant Science*, **283**, 301-310. https://doi.org/10.1016/j.plantsci.2019.03.013

[12] Kluza, A., Wojdyła, Z., Mrugala, B., Kurpiewska, K., Porebski, P.J., Niedzialkowska, E., Minor, W., Weiss, M.S., Borowski, T., Wojdyla, Z., Mrugala, B., Kurpiewska, K., Porebski, P.J., Niedzialkowska, E., Minor, W., Weiss, M.S. and Borowski, T. (2020) Regioselectivity of Hyoscyamine 6β-Hydroxylase-Catalysed Hydroxylation as Revealed by High-Resolution Structural Information and QM/MM Calculations. *Dalton Transactions*, **49**, 4454-4469. https://doi.org/10.1039/D0DT00302F

[13] Grabherr, M.G., Haas, B.J., Yassour, M., Levin, J.Z., Thompson, D.A., Amit, I., Adiconis, X., Fan, L., Raychowdhury, R., Zeng, Q., Chen, Z., Mauceli, E., Hacohen, N., Gnirke, A., Rhind, N., di Palma, F., Birren, B.W., Nusbaum, C., Lindblad-Toh, K., Friedman, N. and Regev, A. (2011) Trinity: Reconstructing a Full-Length Transcriptome without a Genome from RNA-Seq Data. *Nature Biotechnology*, **29**, 644-652. https://doi.org/10.1038/nbt.1883

[14] Bolger, A.M., Lohse, M. and Usadel, B. (2014) Trimmomatic: A Flexible Trimmer for Illumina Sequence Data. *Bioinformatics*, **30**, 2114-2120. https://doi.org/10.1093/bioinformatics/btu170

[15] Li, Q., Zhu, T., Zhang, R., Bu, Q., Yin, J., Zhang, L. and Chen, W. (2020) Molecular Cloning and Functional Analysis of Hyoscyamine 6β-Hydroxylase (H6H) in the Poisonous and Medicinal Plant *Datura innoxia* Mill. *Plant Physiology and Biochemistry*, **153**, 11-19. https://doi.org/10.1016/j.plaphy.2020.04.021

[16] Waterhouse, A., Bertoni, M., Bienert, S., Studer, G., Tauriello, G., Gumienny, R., Heer, F.T., de Beer, T.A.P., Rempfer, C. and Bordoli, L. (2018) SWISS-MODEL: Homology Modelling of Protein Structures and Complexes. *Nucleic Acids Research*, **46**, W296-W303. https://doi.org/10.1093/nar/gky427

[17] Morris, G.M., Huey, R., Lindstrom, W., Sanner, M.F., Belew, R.K., Goodsell, D.S. and Olson, A.J. (2009) AutoDock4 and AutoDockTools4: Automated Docking with Selective Receptor Flexibility. *Journal of Computational Chemistry*, **30**, 2785-2791. https://doi.org/10.1002/jcc.21256

[18] Wallace, A.C., Laskowski, R.A. and Thornton, J.M. (1995) LIGPLOT: A Program to Generate Schematic Diagrams of Protein-Ligand Interactions. *Protein Engineering, Design and Selection*, **8**, 127-134. https://doi.org/10.1093/protein/8.2.127

[19] Schrödinger, L.L.C. (2017) The PyMOL Molecular Graphics System.

[20] Wu, T., Zhu, J.X., Wei, Q., Li, P., Wang, L.B., Huang, J., Wang, J.H., Tang, L.K., Wu, L.J., Li, C. and Han, W.N. (2019) Preparative Separation of Four Isomers of Synthetic Anisodamine by HPLC and Diastereomer Crystallization. *Chirality*, **31**, 11-20. https://doi.org/10.1002/chir.23026

[21] Hashimoto, T., Matsuda, J. and Yamada, Y. (1993) Two-Step Epoxidation of Hyoscyamine to Scopolamine Is Catalyzed by Bifunctional Hyoscyamine 6β-Hydroxylase. *FEBS Letters*, **329**, 35-39. https://doi.org/10.1016/0014-5793(93)80187-Y

[22] Liu, T., Zhu, P., Cheng, K., Meng, C. and He, H.-X. (2005) Molecular Cloning, Expression and Characterization of Hyoscyamine 6β-Hydroxylase from Hairy Roots of *Anisodus tanguticus*. *Planta Medica*, **71**, 249-253. https://doi.org/10.1055/s-2005-837825

[23] Fischer, C., Kwon, M., Ro, D.-K.K., van Belkum, M.J. and Vederas, J.C. (2018) Isolation, Expression and Biochemical Characterization of Recombinant Hyoscyamine-6β-Hydroxylase from: *Brugmansia sanguinea*-Tuning the Scopolamine Production. *MedChemComm*, **9**, 888-892. https://doi.org/10.1039/C8MD00090E

[24] Pramod, K.K., Singh, S. and Jayabaskaran, C. (2010) Biochemical and Structural Characterization of Recombinant Hyoscyamine 6beta-Hydroxylase from *Datura metel* L. *Plant Physiology and Biochemistry*, **48**, 966-970. https://doi.org/10.1016/j.plaphy.2010.09.003

[25] Li, J., van Belkum, M.J. and Vederas, J.C. (2012) Functional Characterization of Recombinant Hyoscyamine 6β-Hydroxylase from *Atropa belladonna*. *Bioorganic & Medicinal Chemistry*, **20**, 4356-4363. https://doi.org/10.1016/j.bmc.2012.05.042

[26] Farrow, S.C. and Facchini, P.J. (2014) Functional Diversity of 2-Oxoglutarate/Fe(II)-Dependent Dioxygenases in Plant Metabolism. *Frontiers in Plant Science*, **5**, 1-15.

https://doi.org/10.3389/fpls.2014.00524

[27] Matsuda, J., Hashimoto, T. and Yamada, Y. (1997) Analysis of Active-Site Residues in Hyoiscyamin 6ß-Hydroxylase. *Plant Biotechnology*, **14**, 51-57. https://doi.org/10.5511/plantbiotechnology.14.51

[28] Aravind, L. and Koonin, E.V. (2001) The DNA-Repair Protein AlkB, EGL-9, and Leprecan Define New Families of 2-Oxoglutarate- and Iron-Dependent Dioxygenases. *Genome Biology*, **2**, research0007.1-0007.8. https://doi.org/10.1186/gb-2001-2-3-research0007

[29] Martinez, S. and Hausinger, R.P. (2015) Catalytic Mechanisms of Fe(II)- and 2-Oxoglutarate-Dependent Oxygenases. *Journal of Biological Chemistry*, **290**, 20702-20711. https://doi.org/10.1074/jbc.R115.648691